Unimolecular Reactions of Ionized Alkanes: Theoretical Study of the Potential Energy Surface for $CH_3^•$ and CH_4 Losses from Ionized Butane and Isobutane

Santiago Olivella,*,† Albert Solé,† David J. McAdoo,*,‡ and Lawrence L. Griffin§

Contribution from the Departaments de Química Orgànica i Química Física, Universitat de Barcelona, Martí i Franquès 1, 08028 Barcelona, Catalunya, Spain, Marine Biomedical Institute, University of Texas Medical Branch, Galveston, Texas 77555-0843, and Department of Marine Sciences, Texas A&M University at Galveston, Galveston, Texas 77553

Received January 24, 1994®

Abstract: In connection with the observed losses of $CH_3^•$ and CH_4 from ionized butane (**1**) and isobutane (**2**) in the gas phase, ab initio molecular orbital calculations at the UMP2, QCISD, and QCISD(T) levels of theory with the 6-31G(d) and 6-31G(d,p) basis sets have been used to investigate the relevant parts of the $C_4H_{10}^{•+}$ ground-state potential energy surface. The isomerization of **1** to **2** is found to take place via a transition structure (**X**) consisting of a nonclassical H-bridged propyl cation coordinated to the methyl radical. **X** lies 19.9 kcal/mol above the lowest-energy trans conformer of **1** and 3.6 kcal/mol above the energy of the dissociation fragments *sec*-propyl cation plus methyl radical. In addition to mediating the **1** → **2** isomerization, **X** also mediates the losses of both $CH_3^•$ and CH_4 from **1** through non-minimum energy reaction paths which are energetically accessible. The CH_4 elimination from **2** is found to take place via a transition structure (**XI**) which can be viewed as a *sec*-propyl cation coordinated to the methyl radical. **XI** is calculated to lie 12.9 kcal/mol above **2** and 3.1 kcal/mol below the energy of its loosely bound components. These theoretical results are consistent with mass spectrometry experimental findings reported in the literature.

I. Introduction

The unimolecular reactions of ionized alkanes are of fundamental interest in gas-phase chemistry.[1-17] Although the chemistry of alkanes is generally regarded as being simple, because of the absence of functional groups, this is not true for the ionized compounds. Extremely complex behavior is frequently observed, even for relatively small $C_nH_{2n+2}^{•+}$ species; loss of alkyl radicals and alkane molecules, often in competition, are common decomposition channels for the molecular ions of saturated hydrocarbons. A variety of rationalizations have been offered to explain the dissociations of ionized alkanes. Wolkoff and Holmes[7] concluded from appearance energy measurements that *n*-alkane molecular ions form secondary carbonium ions rather than the anticipated primary ions upon loss of their terminal methyl groups. They suggested that isomerization of *n*- to *sec*-alkyl ions occurs before or during the loss of methyl radical. They also reported that about 7% of the methyl radical lost from metastable butane radical cations (**1**) comes from within the hydrocarbon chain, again to form secondary carbonium ions. Loss of methyl radical from within the chain could readily be explained by postulating isomerization of **1** to isobutane radical cation (**2**) prior to all losses of the terminal methyl groups. Since that would have given a 1:2 ratio of internal to external origin of methyl radical, they concluded that a 1,2-hydrogen shift occurs in concert with terminal methyl loss. The loss of a methyl bearing an internal carbon atom was attributed to partial isomerization of **1** to **2** or to concerted loss of CH_2 together with an adjacent H atom. This extrusion process is without mechanistic precedent in organic chemistry. Some loss of methane from **1** containing an internal methylene was also observed, which they attributed to decomposition by 1,2-molecular elimination following isomerization of **1** to **2**. In a later study, Holmes and co-workers[13] proposed that fragmentations of **1** by loss of methyl radical and methane proceeded via concerted reactions rather than by a stepwise mechanism in which the energy-rich radical cation **2** participated as a discrete reaction intermediate.

Derrick and co-workers[10] interpreted the very strong secondary isotope effects associated with loss of variously deuterated

† Universitat de Barcelona.
‡ University of Texas Medical Branch.
§ Texas A&M University.
® Abstract published in *Advance ACS Abstracts*, October 15, 1994.

(1) Bursey, J. T.; Bursey, M. M.; Kingston, G. I. *Chem. Rev.* **1973**, *73*, 191.
(2) Holmes, J. L. In *Mass Spectrometry*; Maccoll, A., Ed.; Butterworths: London, 1975; Vol. 5.
(3) Levsen, K. *Org. Mass Spectrom.* **1975**, *10*, 43.
(4) (a) Derrick, P. J.; Falick, A. M.; Burlingame, A. L. *J. Chem. Soc., Faraday Trans. 2* **1975**, 98. (b) Derrick, P. J.; Falick, A. M.; Burlingame, A. L. *J. Chem. Soc., Faraday Trans. 1* **1975**, 1503.
(5) Levsen, K.; Heimbach, H.; Shaw, G. J.; Milne, G. W. A. *Org. Mass Spectrom.* **1977**, *12*, 663.
(6) (a) Lavanchi, A.; Houriet, R.; Gäumann, T. *Org. Mass Spectrom.* **1978**, *13*, 410. (b) Lavanchi, A.; Houriet, R.; Gäumann, T. *Org. Mass Spectrom.* **1979**, *14*, 79.
(7) Wolkoff, P.; Holmes, J. L. *J. Am. Chem. Soc.* **1978**, *100*, 7346.
(8) Holmes, J. L.; Wolkoff, P. *J. Chem. Soc., Chem. Commun.* **1979**, 544.
(9) Bowen, R. D.; Barbalas, M. P.; Pagano, F. P.; Todd, P. J.; McLafferty, F. W. *Org. Mass Spectrom.* **1980**, *15*, 51.
(10) Mead, P. T.; Donchi, K. F.; Traeger, J. C.; Christie, J. R.; Derrick, P. J. *J. Am. Chem. Soc.* **1980**, *102*, 3364.
(11) Holmes, J. L.; Terlouw, J. K.; Burgers, P. C.; Rye, R. T. B. *Org. Mass Spectrom.* **1980**, *15*, 149.
(12) Wendleboe, R. D.; Bowen, R. D.; Williams, D. H. *J. Am. Chem. Soc.* **1981**, *103*, 2333.
(13) Holmes, J. L.; Burgers, P. C.; Mollah, M. Y. A.; Wolkoff, P. *J. Am. Chem. Soc.* **1982**, *104*, 2879.
(14) Wolkoff, P.; Hammerum, S.; Holmes, J. L. *Int. J. Mass Spectrom. Ion Proc.* **1983**, *47*, 343.
(15) Hudson, C. E.; McAdoo, D. J. *Int. J. Mass Spectrom. Ion Proc.* **1984**, *59*, 325.
(16) (a) Weitzel, K. M.; Booze, J. A.; Baer, T. *Int. J. Mass Spectrom. Ion Proc.* **1991**, *107*, 301. (b) Weitzel, K. M.; Booze, J. A.; Baer, T. *Chem. Phys.* **1991**, *150*, 263.
(17) McAdoo, D. J.; Hudson, C. E. *Rapid Commun. Mass Spectrom.* **1991**, *5*, 357.

0002-7863/94/1516-11078$04.50/0

Scheme 1

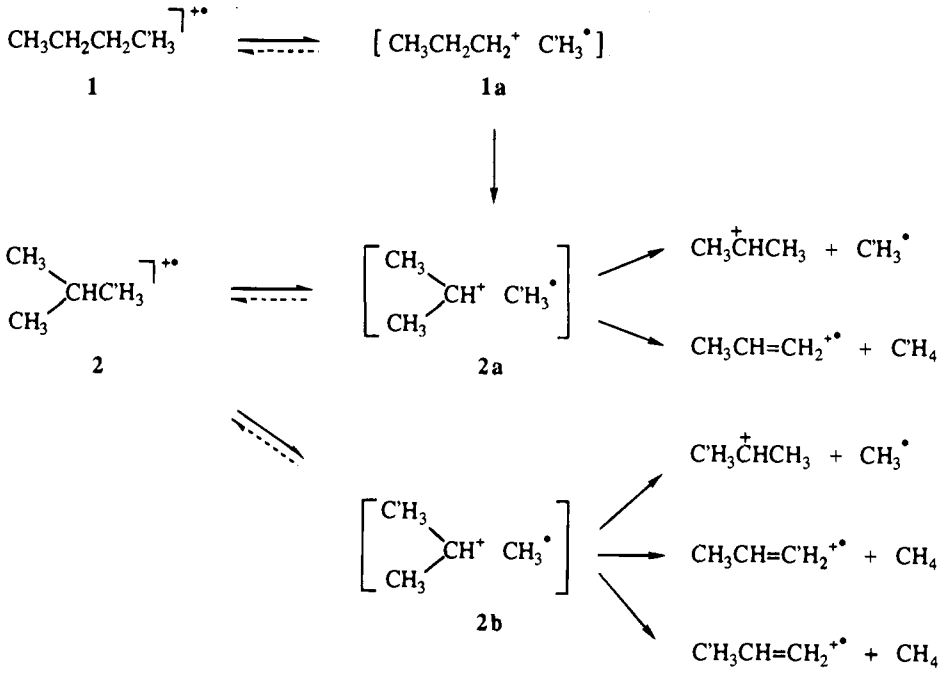

methanes (i.e., CH_3D:CD_3H:CD_4 = 100:12:4.7) from metastable isobutane-*1,1,1,3,3,3-d*$_6$ radical cation ($(CD_3)_2CHCH_3^{\bullet+}$) in terms of a nonclassical transition state involving a three-center bond. These authors concluded that hydrogen transfer is not rate determining and is complete before the transition state is reached. Their proposal cannot account for the interchanges of hydrogen atoms and alkyl groups on adjacent carbon atoms that occur in low-energy alkane ions.[7,12,14]

In 1981, Wendelboe, Bowen, and Williams (WBW)[12] suggested that the dissociations of butane and other ionized alkanes are mediated by ion−neutral complexes, i.e., species in which noncovalent interactions retain close together two entities formed by simple bond cleavages, so that they are able to react unimolecularly (e.g., an incipient cation may isomerize) or bimolecularly (e.g., by hydrogen transfer).[18] Their model rationalizes losses of methyl radical and methane from **1** and **2** as shown in Scheme 1. In this scheme, **1a**, **2a**, and **2b** represent ion−neutral complexes in which an original covalent C−C bond has been effectively broken. These loose complexes of propyl ions and methyl radicals are weakly bound relative to the completely separated carbonium ion and radical. For instance, polarization of the electron cloud of the incipient radical gives rise to weakly bonding ion/induced dipole attractions in **1a**, **2a**, and **2b**. WBW also pointed out that about 16 kcal/mol of energy would be released in the *n*- to *sec*-propyl isomerization, causing such rapid dissociation of the ion−neutral complex that **2** frequently was not fully formed. The appearance energies for the losses of methyl radical and methane from **1** are nearly the same,[7] in contrast to the about 6 kcal/mol lower threshold for the loss of methane than for the loss of methyl radical from **2**.[10] This supports the model in Scheme 1. Decompositions of ionized pentanes and *n*-heptanes were similarly rationalized.[12]

The purpose of the present work is to test theoretically the validity of Scheme 1 by providing a reasonable view of the potential energy surface (PES) associated with the methyl radical and methane losses from ionized butane and isobutane in the gas phase. Therefore, we investigated the $C_4H_{10}^{\bullet+}$ ground-state PES by means of ab initio molecular orbital calculations. In particular, we address the questions related to the geometrical structure and nature (minimum or saddle point) of the stationary points corresponding to the postulated ion−neutral complexes, as well as the mechanisms of the methyl radical and methane eliminations from ionized butane and isobutane. Finally, a comparison is made of the theoretical results with mass spectrometry experiments.

II. Computational Details

The geometries of the stationary points on the electronic $C_4H_{10}^{\bullet+}$ ground-state PES were initially located at the spin-unrestricted Hartree−Fock level of theory[19] employing the split-valence d-polarized 6-31G(d) basis set[20] (UHF/6-31G(d)) and then further optimized at the UMP2/6-31G(d) level, where the effects of dynamical electron correlation were accounted for through full (i.e., not frozen core) second-order Moller−Plesset perturbation theory.[21] The amount of spin contamination in the reference UHF wave function was found to be very small; thus the expectation values of the $\hat{S}^2$ operator were always very close to the value of 0.75 for a pure doublet state, i.e., in a range of 0.755 to 0.765. At the UMP2/6-31G(d) level, the harmonic vibrational frequencies were obtained by diagonalizing the mass-weighted Cartesian force constant matrix, calculated from analytical second derivatives of the total energy, to characterize the stationary points as minima or as saddle points and to facilitate zero-point vibrational energy (ZPVE) corrections to the relative energies. In order to predict more reliable ZPVE values, the raw theoretical harmonic frequencies were scaled by 0.93 to account for their average overestimation at the UMP2/6-31G(d) level of theory.[22] In several cases, intrinsic reaction coordinate (IRC) methods[23] were used to track minimum energy paths from transition structures to their connecting minima. The IRCs were generated in mass-weighted internal coordinates using a step size of 0.3 amu$^{1/2}$ bohr.

(18) (a) Morton, T. H. *Tetrahedron* **1982**, *38*, 3195. (b) McAdoo, D. J. *Mass Spectrom. Rev.* **1988**, *7*, 363. (c) Bouchoux, G. *Adv. Mass Spectrom.* **1989**, *11*, 812. (d) Hammerum, S. In *Fundamentals of Gas Phase Ion Chemistry*; Jennings, K. R., Ed.; Kluwer Academic Publishers: Dordrecht, The Netherlands, 1990; pp 379−390. Bowen, R. D. *Acc. Chem. Res.* **1991**, *24*, 364. (e) Longevialle, P. *Mass Spectrom. Rev.* **1992**, *11*, 157. (f) McAdoo, D. J.; Morton, T. H. *Acc. Chem. Res.* **1993**, *26*, 295.

(19) Pople, J. A.; Nesbet, R. K. *J. Chem. Phys.* **1954**, *22*, 571.

(20) Hariharan, P. C.; Pople, J. A. *Theor. Chim. Acta* **1973**, *28*, 213.

(21) (a) Moller, C.; Plesset, M. *Phys. Rev.* **1934**, *46*, 618. (b) Pople, J. A.; Binkley, J. S.; Seeger, R. *Int. J. Quantum Chem., Symp.* **1976**, *10*, 1.

(22) (a) Hout, R. F.; Levi, B. A.; Hehre, W. J. *J. Comput. Chem.* **1982**, *3*, 234. (b) DeFrees, D. J.; McLean, A. D. *J. Chem. Phys.* **1985**, *82*, 333.

(23) (a) Gonzalez, C.; Schlegel, H. B. *J. Chem. Phys.* **1989**, *90*, 2154. (b) Gonzalez, C.; Schlegel, H. B. *J. Phys. Chem.* **1990**, *94*, 5523.

At geometries optimized using the UMP2/6-31G(d) wave function, the energies were recalculated using (frozen core) the quadratic configuration interaction with singles, doubles, and perturbative estimation of triples method[24] (QCISD(T)) employing the split-valence d,p-polarized 6-31G(d,p) basis set.[20] Our best relative energies correspond to the QCISD(T)/6-31G(d,p) level together with the ZPVE correction calculated at the UMP2/6-31G(d) level. Unless otherwise noted, these are the values given in the text.

Basis set superposition errors (BSSE) are expected to affect the computed interaction in electrostatically bound species.[25] However, it has been shown that these effects, although they tend to overestimate the ion−neutral complex stability relative to that of the completely separated components, are not very pronounced and do not exceed 1−2 kcal/mol.[26]

The charge and spin density distributions of the most relevant structures were examined by means of the Mulliken population analysis[27] of the **Z** density matrix obtained from UMP2 (full) gradient calculations with the 6-31G(d,p) basis set, an effective correlated density matrix which represents the response of the correlated system to any one-electron correlation.[28]

The dependence of the unimolecular rate constant $k(E)$ on the internal energy E of a reactant ion was calculated on the basis of standard RRKM theory of unimolecular reactions, which can be formulated as[29]

$$k(E) = \frac{W^{\dagger}(E)}{h\varrho(E)} \qquad (1)$$

where $W^{\dagger}(E)$ is the total number of states of the transition state with energy less than or equal to E, $\varrho(E)$ is the density of states of the reactant ion, and h is Planck's constant. $W^{\dagger}(E)$ and $\varrho(E)$ were enumerated by direct count of vibrational states using a program[30] based on the Beyer−Swinehart algorithm.[29,31] The RRKM computations employed the potential energy barriers calculated at the QCISD(T)/6-31G(d,p) level and the UMP2/6-31G(d)-calculated harmonic vibrational frequencies scaled by the factor 0.93.

All of the ab initio calculations described here were performed with the GAUSSIAN 90[32] and GAUSSIAN 92[33] series of programs, running on a CRAY Y-MP8/864 computer at the CHPC in Austin and a CRAY Y-MP2/32 computer at the CESCA in Barcelona.

III. Results and Discussion

The most relevant geometrical parameters of the optimized molecular structures computed for the stationary points located on the $C_4H_{10}^{\bullet+}$ ground-state PES concerning **1**, **2**, the isomerization of **1** to **2**, and the methane elimination from **2** are given in Figures 1−7, which are computer plots of the UMP2/6-31G(d)-optimized geometries. The full optimized geometries are available as supplementary material. The total and relative energies, calculated at various levels of theory, are shown in Tables 1 and 2. The ZPVE, computed from the scaled vibrational frequencies, have been included in Table 2. Finally, the total atomic charges and spin densities of the most relevant structures are shown in Tables 3 and 4, respectively.

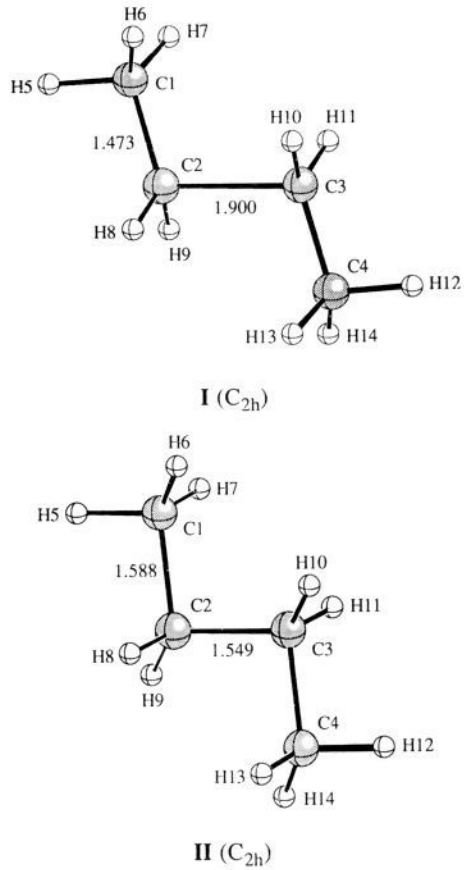

Figure 1. UMP2/6-31G(d)-optimized structures of the stationary points **I** and **II** on the $C_4H_{10}^{\bullet+}$ ground-state PES.

A. Butane Radical Cation. In agreement with previous semiempirical[34] and ab initio calculations,[35,36] the lowest-energy minimum found on the ground-state PES concerning **1** has C_{2h} symmetry. It corresponds to the trans conformation of **1** and its electronic wave function has ^2A_g symmetry. The optimized geometry of this minimum, **I** (Figure 1), shows a central C−C bond distance of 1.900 Å and two terminal C−C bond distances of 1.473 Å, which are 0.375 Å longer and 0.051 Å shorter, respectively, than the corresponding C−C bond distances (1.525 and 1.524 Å) calculated at the same level of theory for neutral butane.[37] This predicted substantial change in structure accompanying ionization of neutral butane is consistent with the observed large difference (i.e., 0.7−0.6 eV) between the vertical and adiabatic ionization potentials.[38]

(24) Pople, J. A.; Head-Gordon, M.; Raghavachari, K. *J. Chem. Phys.* **1987**, *87*, 5968.

(25) See, for example: (a) Urban, M.; Hozba, P. *Theor. Chim. Acta* **1975**, *36*, 215. (b) Ostlund, N. S.; Merrifield, D. L. *Chem. Phys. Lett.* **1976**, *39*, 612. (c) Bulski, H.; Chalasinski, G. *Theor. Chim. Acta* **1977**, *44*, 399. (d) Kolos, W. *Theor. Chim. Acta* **1979**, *51*, 219. (e) Leclercq, J. M.; Allavena, M.; Bouteilleur, Y. *J. Chem. Phys.* **1983**, *78*, 4606. (f) Hobza, P.; Zahradnik, R. *Int. J. Quantum Chem.* **1983**, *23*, 325. (g) Wells, B. H.; Wilson, S. *Chem. Phys. Lett.* **1983**, *101*, 429.

(26) (a) Latajka, Z.; Scheiner, S. *Chem. Phys.* **1985**, *98*, 59. (b) Postma, R.; Ruttink, P. J. A.; van Baar, B.; Terlouw, J. K.; Holmes, J. L.; Burgers, P. C. *Chem. Phys. Lett.* **1986**, *123*, 409.

(27) Mulliken, R. S. *J. Chem. Phys.* **1955**, *23*, 1833.

(28) See, for example: Wiberg, K. B.; Hadad, C. M.; LePage, T.; Breneman, C. M.; Frisch, M. J. *J. Phys. Chem.* **1992**, *96*, 671.

(29) Gilbert, R. G.; Smith, S. C. *Theory of Unimolecular and Recombination Reactions*; Blackwell Scientific Publications: Oxford, 1990.

(30) Solé, A., unpublished work.

(31) Beyer, T.; Swineheart, D. F. *Comm. Ass. Comput. Machines* **1973**, *16*, 379.

(32) Frisch, M. J.; Head-Gordon, M.; Trucks, G. W.; Foresman, J. B.; Schlegel, H. B.; Raghavachari, K.; Robb, M.; Binkley, J. S.; Gonzalez, C.; Defrees, D. J.; Fox, D. J.; Whiteside, R. A.; Seeger, R.; Melius, C. F.; Baker, J.; Martin, R. L.; Kahn, L. R.; Stewart, J. J. P.; Topiol, S.; Pople, J. A. *GAUSSIAN 90*; Gaussian Inc.: Pittsburgh, PA, 1990.

(33) Frisch, M. J.; Trucks, G. W.; Head-Gordon, M.; Gill, P. M. W.; Wong, M. W.; Foresman, J. B.; Johnson, B. G.; Schlegel, H. B.; Robb, M. A.; Replogle, E. S.; Gomperts, R.; Andres, J. L.; Raghavachari, K.; Binkley, J. S.; Gonzalez, C.; Martin, R. L.; Fox, D. J.; Defrees, D. J.; Baker, J.; Stewart, J. J. P.; Pople, J. A. *GAUSSIAN 92*; Gaussian, Inc.: Pittsburgh, Pa, 1992.

(34) Bellville, D. J.; Bauld, N. L. *J. Am. Chem. Soc.* **1982**, *104*, 5700.

(35) (a) Takeuchi, T.; Yamamoto, M.; Nishimoto, K.; Tanaka, H.; Hirota, K. *Int. J. Mass Spectrom. Ion Phys.* **1983**, *52*, 139. (b) Bouma, W. J.; Poppinger, D.; Radom, L. *Isr. J. Chem.* **1983**, *23*, 21.

(36) (a) Huang, M.-B.; Lunell, S. *J. Mol. Struct. (THEOCHEM)* **1990**, *205*, 317. (b) Lunell, S.; Eriksson, L. A.; Worsbrock, L. *J. Am. Chem. Soc.* **1991**, *113*, 7508.

(37) Olivella, S.; Solé, A., unpublished work.

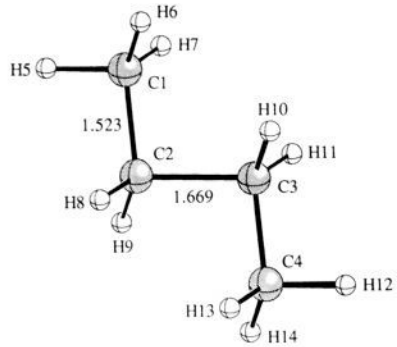

III (C_{2h})

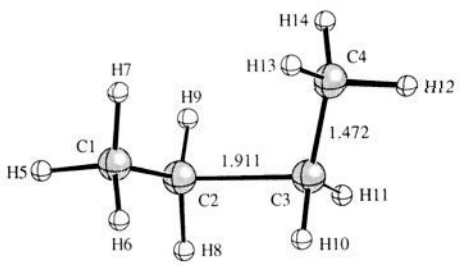

IV (C_2)

Figure 2. UMP2/6-31G(d)-optimized structures of the stationary points **III** and **IV** on the $C_4H_{10}^{\bullet+}$ ground-state PES.

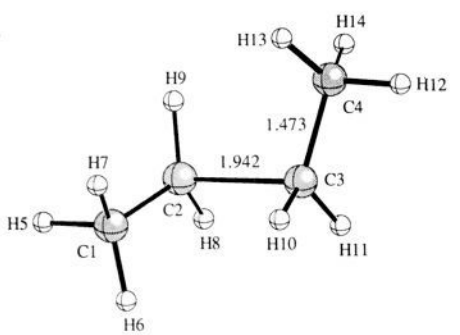

V (C_2)

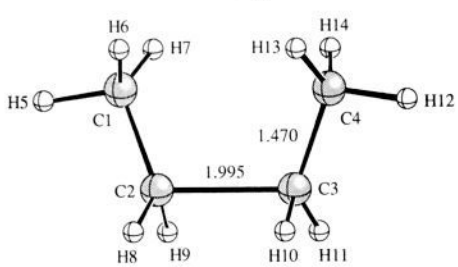

VI (C_{2v})

Figure 3. UMP2/6-31G(d)-optimized structures of the stationary points **V** and **VI** on the $C_4H_{10}^{\bullet+}$ ground-state PES.

Another C_{2h} local minimum was found on the same PES at which the electronic wave function again has ^2A_g symmetry. The optimized geometry of this second minimum, **II** (Figure 1), has a central C−C bond distance of 1.549 Å and two terminal C−C bonds of 1.588 Å. It is worth noting that the initial UHF/6-31G(d) calculations gave for this second minimum of the trans conformation a C_s structure showing a long (1.982 Å) and a normal (1.559 Å) terminal C−C bond, while the central C−C bond has a length of 1.484 Å. This spurious geometry indicates that the UHF theory is not suitable for computing reliable molecular geometries of alkane radical cations and points out the necessity of including electron correlation in the quantum-mechanical method used to perform the geometry optimization of these species. At the UMP2/6-31G(d) level, **II** is higher in energy than **I** by 1.2 kcal/mol and both minima are connected by a C_{2h} saddle point lying 1.5 kcal/mol above **I**. The optimized geometry of this transition structure, **III** (Figure 2), has a central C−C bond distance of 1.669 Å and two terminal C−C bonds of 1.523 Å. It is worthwhile to note that the relative energies of the stationary points **I**−**III** are sensitive to the method used to calculate the electron correlation correction. In particular, with the 6-31G(d,p) basis set, at the UMP2 level of theory the

(38) Experimental value for the vertical ionization potential of butane: 11.2 eV.[39a] Experimental values for the adiabatic ionization potential of butane: 10.50,[39b] 10.6,[39a] and 10.63 eV.[39c]

(39) (a) Bieri, G.; Burger, F.; Heilbroner, E.; Maier, J. P. *Helv. Chim. Acta* **1978**, *100*, 7346. (b) Al-Joboury, M. I.; Turner, D. W. **1964**, *J. Chem. Soc. B* 4434. (c) Watanabe, K. *J. Chem. Phys.* **1957**, *26*, 242.

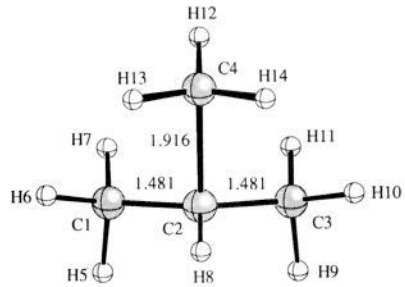

VII (C_s)

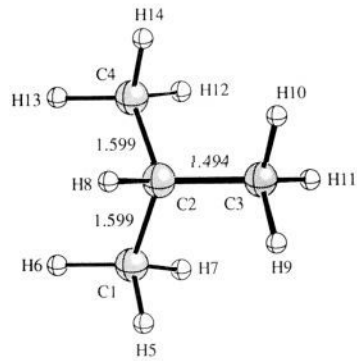

VIII (C_s)

Figure 4. UMP2/6-31G(d)-optimized structures of the stationary points **VII** and **VIII** on the $C_4H_{10}^{\bullet+}$ ground-state PES.

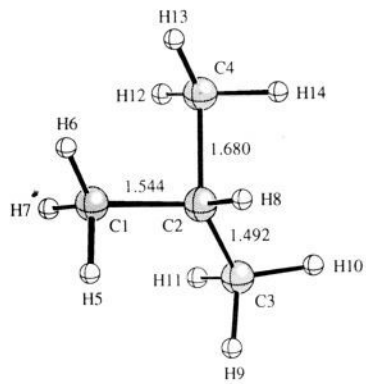

IX (C_1)

Figure 5. UMP2/6-31G(d)-optimized structures of the stationary point **IX** on the $C_4H_{10}^{\bullet+}$ ground-state PES.

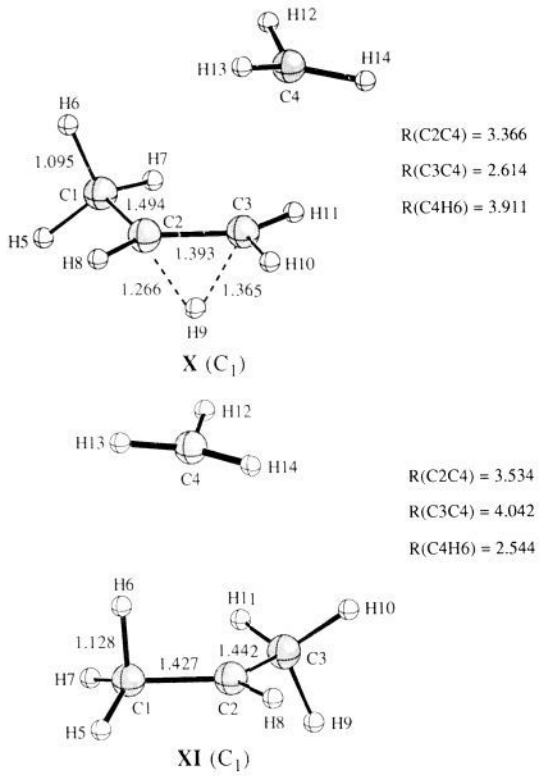

Figure 6. UMP2/6-31G(d)-optimized structures of the stationary points **X** and **XI** on the $C_4H_{10}^{\bullet+}$ ground-state PES.

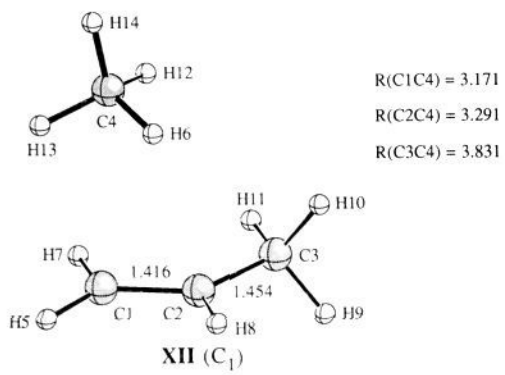

Figure 7. UMP2/6-31G(d)-optimized structures of the stationary point **XII** on the $C_4H_{10}^{\bullet+}$ ground-state PES.

equilibrium structure **II** is predicted to lie 0.4 kcal/mol below the transition structure **III**, whereas at the QCISD and QCISD(T) levels **II** is found to lie 1.4 and 1.0 kcal/mol, respectively, *above* **III**. This indicates that the molecular geometries calculated for **II** and **III** depend on the amount of electron correlation included in the quantum-mechanical method used to optimize the geometry of these structures. Therefore, a meaningful evaluation of the relative energies of structures **I**−**III** at a given level of theory should be done using the geometries optimized at the same level. Due to the prohibitive computational cost involved, the geometry re-optimization of structures **I**−**III** at the QCISD(T) level was not attempted in the present study.[40]

As was previously found by Lunell and co-workers,[36] a C_2 minimum was located on the ground-state PES whose wave function has ^2A symmetry. This local minimum is the gauche conformation of **1** and its optimized geometry, **IV** (Figure 2), has a central C−C bond distance of 1.911 Å and two peripheral C−C bond distances of 1.472 Å, which are nearly identical to the C−C bond distances calculated for the trans conformation (**I**). At the UMP2/6-31G(d) level, this gauche conformation is predicted to be only 0.3 kcal/mol more energetic than the trans conformation. A saddle point of C_2 symmetry linking the minima **I** and **IV** was also located on the same PES. Its optimized geometry, **V** (Figure 3), has a central C−C bond distance of 1.942 Å and two terminal C−C bond distances of 1.473 Å. At the UMP2/6-31G(d) level, **V** lies 2.1 kcal/mol above **I**. Further, a stationary point of C_{2v} symmetry was also found on the ground-state PES at which the wave function has $^2A_1$ symmetry. This point is the cis conformation of **1**, and its optimized geometry, **VI** (Figure 3), has a central C−C bond distance of 1.995 Å and two terminal C−C bond distances of 1.470 Å. The vibrational analysis proved **VI** to be the transition structure interconverting the two equivalent gauche conformations of **1** by rotation of the two terminal C−C bonds around the central C−C bond in **IV**. At the UMP2/6-31G(d) level, the potential energy barrier for this rotational process is calculated to be 3.2 kcal/mol.

At our best level of theory, namely, QCISD(T)/6-31G(d,p), the computed relative energies (in kcal/mol) calculated for the above stationary points are the following: 0.0 (**I**), 3.5 (**II**), 2.5 (**III**), 0.4 (**IV**), 2.0 (**V**), and 3.5 (**VI**). Inclusion of the ZPVE correction in the latter relative energies leads to our final values of 0.0 (**I**), 4.0 (**II**), 2.2 (**III**), 0.5 (**IV**), 2.0 (**V**), and 3.5 (**VI**) kcal/mol.

B. Isobutane Radical Cation. As was previously found by Radom and co-workers,[35b] the lowest-energy minimum calculated on the ground-state PES concerning **2** has C_s symmetry and its electronic wave function has $^2A'$ symmetry. The optimized structure of this point, **VII** (Figure 4), has a C−C bond distance of 1.916 Å and two C−C bond distances of 1.481 Å, which are 0.390 Å longer and 0.045 Å shorter, respectively, than the value (1.526 Å) calculated at the same level of theory for the three C−C bonds of neutral isobutane.[37] Again, this marked change in structure accompanying ionization of neutral isobutane reflects the observed large difference (i.e., 0.7−0.22 eV) between the vertical and adiabatic ionization potentials.[42] At the QCISD(T)/6-31G(d,p)+ZPVE level of theory the energy difference between **VII** and **I** is calculated to be 0.3 kcal/mol, compared to an experimental value of −1.0 kcal/mol.[43] It is noteworthy that at the same level of theory neutral isobutane is calculated as 1.6 kcal/mol *less* energetic than the trans conformation of neutral butane.[37] This energy difference is reasonably close to the experimental estimate of 2.1 kcal/mol.[45]

Another C_s local minimum was found on the ground-state PES of **2** at which the electronic wave function has $^2A''$

(40) A reviewer has pointed out that the two orbitals describing the C−C−C−C part of **I** and **II** might be degenerate or near-degenerate and recommended complete active space self-consistent field (CASSCF) calculations to probe this question further. To determine the orbitals which define the hypothetical "active space" of **I**−**III**, we have calculated the natural orbitals of the UHF/6-31G(d) wave function (UNOs) of these structures. According to Pulay and Hamilton,[41] the "active space" should include the UNOs with significant fractional occupation, say between 0.02 and 1.98. In the case of structures **I**−**III** it turned out that there was not any significant fractional occupancy of the UNOs. This indicates that there are not "active" orbitals, beside the orbital describing the unpaired electron, and rules out the necessity of performing CASSCF calculations on these structures.

(41) Pulay, P.; Hamilton, T. P. *J. Chem. Phys.* **1988**, *88*, 4926.

(42) Experimental value for the vertical ionization potential of isobutane: 11.0 eV.[39a] Experimental values for the adiabatic ionization potential of isobutane: 10.3[39a] and 10.78 eV.[39b]

(43) Estimated from $\Delta H^\circ_f(\mathbf{1}) = 212.5$ kcal/mol and $\Delta H^\circ_f(\mathbf{2}) = 211.5$ kcal/mol at 298 K.[44]

(44) Lias, S. G.; Bartmess, J. E.; Liebman, J. B.; Holmes, J. L.; Levin, R. D.; Mallard, W. G. *J. Phys. Chem. Ref. Data* **1988**, *17*, 168.

(45) Obtained from $\Delta H^\circ_f(n\text{-}C_4H_{10}) = -30.0$ kcal/mol and $\Delta H^\circ_f(i\text{-}C_4H_{10}) = -32.1$ kcal/mol at 298 K.[46]

Table 1. Total Energies (in au)[a] and Zero-Point Vibrational Energies (ZPVE, in kcal/mol)[b] of the Stationary Points Calculated on the $C_4H_{10}^{\bullet+}$ Potential Energy Surface

structure	point group	state	UMP2/6-31G(d)	UMP2[c]/6-31G(d,p)	QCISD[c]/6-31G(d,p)	QCISD(T)[c]/6-31G(d,p)	ZPVE
I	C_{2h}	$^2A_{1g}$	−157.468 82	−157.527 27	−157.590 82	−157.607 76	76.2
II	C_{2h}	$^2A_{1g}$	−157.466 90	−157.525 14	−157.583 00	−157.602 17	76.7
III	C_{2h}	$^2A_{1g}$	−157.466 43	−157.524 62	−157.585 30	−157.603 79	75.9
IV	C_2	^2A	−157.468 29	−157.526 82	−157.590 21	−157.607 18	76.3
V	C_2	^2A	−157.465 55	−157.524 05	−157.587 68	−157.604 64	76.2
VI	C_{2v}	$^2A_1$	−157.463 24	−157.521 83	−157.585 34	−157.602 22	76.2
VII	C_s	$^2A'$	−157.468 47	−157.526 84	−157.589 98	−157.606 99	76.0
VIII	C_s	$^2A''$	−157.464 61	−157.522 84	−157.582 28	−157.600 82	76.1
IX	C_1	^2A	−157.464 37	−157.522 62	−157.583 27	−157.601 54	75.7
X	C_1	^2A	−157.431 04	−157.491 57	−157.554 39	−157.571 19	73.2
XI	C_1	^2A	−157.440 77	−157.499 32	−157.564 46	−157.580 03	72.0
XII	C_1	^2A	−157.467 73	−157.526 70	−157.592 49	−157.607 82	74.0
$(CH_3)_2CH^+$	C_2	^1A	−117.760 65	−117.799 54	−117.844 27	−117.856 95	53.0
$CH_3^{\bullet}$	D_{3h}	$^2A_2''$	−39.673 03	−39.692 67	−39.713 72	−39.716 23	17.8
$CH_3CH{=}CH_2^{\bullet+}$	C_s	$^2A''$	−117.126 87	−117.158 09	−117.202 77	−117.214 19	46.2
CH_4	T_d	$^1A_1$	−40.337 04	−40.364 58	−40.386 12	−40.389 59	27.1

[a] Based on the UMP2/6-31G(d)-optimized geometries. [b] Calculated from the UMP2/6-31G(d) frequencies scaled by the factor 0.93. [c] In the frozen core approximation.

Table 2. Relative Energies (in kcal/mol)[a] of the Stationary Points Calculated on the $C_4H_{10}^{\bullet+}$ Potential Energy Surface at Various Levels of Theory

structure	UMP2/6-31G(d)	UMP2[b]/6-31(d,p)	QCISD[b]/6-31G(d,p)	QCISD(T)[b]/6-31G(d,p)	QCISD(T)[b]/6-31G(d,p)+ZPVE	exp[c]
I	0.0	0.0	0.0	0.0	0.0	0.0
II	1.2	1.3	4.9	3.5	4.0	
III	1.5	1.7	3.5	2.5	2.2	
IV	0.3	0.3	0.4	0.4	0.5	
V	2.1	2.0	2.0	2.0	2.0	
VI	3.5	3.4	3.4	3.5	3.5	
VII	0.2	0.3	0.5	0.5	0.3	−1.0
VIII	2.6	2.8	5.4	4.4	4.3	
IX	2.8	2.9	4.7	3.9	3.4	
X	23.7	22.4	22.9	22.9	19.9	
XI	17.4	17.5	16.5	17.4	13.2	
XII	0.7	0.3	−1.0	0.0	−2.2	
$(CH_3)_2CH^+ + CH_3^{\bullet}$	22.1	22.0	20.6	21.7	16.3	13.2
$CH_3CH{=}CH_2^{\bullet+} + CH_4$	3.1	2.9	2.1	2.5	−0.4	−1.3

[a] Based on the UMP2/6-31G(d)-optimized geometries. [b] In the frozen core approximation. [c] Estimated from the heats of formation at 298 K of ref 44.

Table 3. Total Atomic Charges of Several Stationary Points Calculated on the $C_4H_{10}^{\bullet+}$ Potential Energy Surface[a,b]

atom	**I**	**VII**	**X**	**XI**	$(CH_3)_2CH^+$	$CH_3^{\bullet}$
C1	−0.394	−0.374	−0.389	−0.443	−0.451	
C2	−0.192	−0.128	−0.121	+0.164	+0.168	
C3	−0.192	−0.374	−0.190	−0.447	−0.451	
C4	−0.394	−0.270	−0.412	−0.430		−0.374
H5	+0.230	+0.225	+0.205	+0.241	+0.246	
H6	+0.195	+0.192	+0.211	+0.257	+0.263	
H7	+0.195	+0.190	+0.177	+0.228	+0.228	
H8	+0.232	+0.243	+0.255	+0.256	+0.261	
H9	+0.232	+0.225	+0.252	+0.255	+0.263	
H10	+0.232	+0.192	+0.257	+0.239	+0.246	
H11	+0.232	+0.190	+0.250	+0.219	+0.228	
H12	+0.230	+0.230	+0.165	+0.152		+0.125
H13	+0.195	+0.231	+0.167	+0.161		+0.125
H14	+0.195	+0.231	+0.174	+0.148		+0.125

[a] Determined from the Mulliken population analysis of the **Z** density matrix obtained from UMP2(full)/6-31G(d,p) gradient calculations. [b] Atom numberings refer to Figures 1, 4, and 6.

Table 4. Total Atomic Spin Densities of Several Stationary Points Calculated on the $C_4H_{10}^{\bullet+}$ Potential Energy Surface[a,b]

atom	**I**	**VII**	**X**	**XI**	$CH_3^{\bullet}$
C1	−0.006	−0.013	−0.002	+0.011	
C2	+0.446	+0.350	+0.030	+0.002	
C3	+0.446	−0.013	+0.049	0.000	
C4	−0.006	+0.581	+1.054	+1.140	+1.198
H5	+0.068	+0.061	+0.001	0.000	
H6	+0.005	+0.004	+0.003	+0.019	
H7	+0.005	+0.005	0.000	0.000	
H8	−0.009	0.000	−0.002	0.000	
H9	−0.009	+0.061	+0.024	0.000	
H10	−0.009	+0.004	−0.004	0.000	
H11	−0.009	+0.005	−0.004	0.000	
H12	+0.068	−0.016	−0.050	−0.057	−0.066
H13	+0.005	−0.015	−0.050	−0.057	−0.066
H14	+0.005	−0.015	−0.049	−0.057	−0.066

[a] Determined from the Mulliken population analysis of the **Z** density matrix obtained from UMP2(full)/6-31(d,p) gradient calculations. [b] Atom numberings refer to Figures 1, 4, and 6.

symmetry. This is in accord with the previous work of Radom and co-workers.[35b] The optimized geometry of this second minimum, **VIII** (Figure 4), has two elongated C−C bonds showing a length of 1.599 Å and a somewhat short C−C bond of 1.494 Å. At the UMP2/6-31G(d) level, **VIII** is higher in energy than **VII** by 2.4 kcal/mol. At the latter level of theory, it was found that the interconversion between the equilibrium structures **VII** and **VIII** takes place via the nonsymmetric transition structure **IX** (Figure 5). The atomic displacements associated with the single imaginary frequency (380*i*) of **IX** indicated a shortening of the C2−C4 bond combined with a lengthening of the C1−C2 bond. Furthermore, an IRC calculation starting at the saddle point **IX** confirmed that such a transition structure connects the local minima **VII** and **VIII** on the ground-state PES of **2**.

(46) Pedley, J. B.; Rylance, J. *Computer Analyzed Thermochemical Data: Organic and Organometallic Compounds*; University of Sussex: England, 1977.

According to our results, a degenerate rearrangement **VII** → **VII'**, consisting of the exchange between the long C−C bond and one of the two short C−C bonds in **VII**, takes place via a two-step mechanism which involves the formation of **VIII** as an intermediate along the path **VII** → **IX** → **VIII** → **IX'** → **VII'**. The UMP2/6-31G(d)-calculated potential energy barrier for the conversion of **VII** into **VIII** is only 2.6 kcal/mol, whereas at the QCISD(T)/6-31G(d,p)+ZPVE level of theory the barrier is predicted to be 3.1 kcal/mol. However, as found for the stationary points **I**−**III**, the relative energies of structures **VII**−**IX** are sensitive to the level of theory employed. Thus, with the 6-31G(d,p) basis set, at the UMP2 level of theory the equilibrium structure **VIII** is predicted to lie 0.1 kcal/mol below the transition structure **IX**, whereas at the QCISD and QCISD(T) levels **VIII** is calculated to lie 0.7 and 0.5 kcal/mol, respectively, *above* **IX**. Again, a meaningful evaluation of the relative energies of structures **VII**−**IX** at a given level of theory should be done using the geometries optimized at the same level. Nevertheless, the low energy barrier calculated at all levels of theory used in this study indicates that scrambling of the methyl groups in **2** (i.e., **VII** → **VII'**) should be a facile process.

C. Isomerization of Ionized Butane to Ionized Isobutane. The computation of the minimum energy reaction path (MERP) for methyl radical elimination from **1** was initially attempted by simple elongation of a terminal C−C bond. Starting at the equilibrium structure **IV**, the C3−C4 distance was taken as the reaction coordinate, the energy being minimized with respect to all other geometrical variables without imposing any geometrical restriction. The increase of the C3−C4 distance caused a simultaneous elongation of one of the two adjacent C−H bonds (i.e., C2−H9), so the corresponding hydrogen atom (H9) was moving to the C3 carbon atom along the reaction path. This MERP led eventually to the location of a saddle point at the C3−C4 distance of about 2.6 Å. The transition structure located in this way was refined by minimizing the scalar gradient of the energy using Schlegel's algorithm.[47] The resulting stationary point, **X** (Figure 6), was characterized as a true transition structure by checking that it had only one imaginary harmonic vibrational frequency. The one imaginary frequency (280*i*) corresponded chiefly to a lengthening of the C3−C4 bond combined with a shortening of the C3−H9 distance.

It is worth noting that the propyl moiety of **X** shows a hydrogen atom (H9) simultaneously bonded to the central carbon atom (C2) and to the carbon atom (C3) loosely bound to the methyl moiety. Regarding the charge and spin density distributions (Tables 3 and 4), it is remarkable that the sum of the total atomic charges of the propyl moiety (+0.907) accounts for nearly 91% of the positive charge of **X**, whereas the sum of the total atomic spin densities of the methyl radical moiety (0.905) accounts for nearly 91% of the unpaired electron population of **X**. Therefore, on the basis of the molecular geometry and the total atomic charges and spin densities, the transition structure **X** can be viewed as a nonclassical H-bridged propyl cation coordinated to the methyl radical.

Further increments of the C3···C4 distance in **X** led to a continuous decrease of the C2−C3−C4 angle in the H-bridged propyl cation partner, while the H9 hydrogen atom was progressively shifted to the C3 carbon atom. Furthermore, an IRC calculation beginning at the saddle point **X** and proceeding in the direction corresponding to the elongation of the C3···C4 distance yielded a smooth path leading to the lowest-energy equilibrium structure already calculated for **2**, namely **VII**. Beginning an IRC calculation at **X** and proceeding in the direction corresponding to the shortening of the C3···C4 bond a smooth path leading to the equilibrium structure calculated for the gauche conformation of **1** (**IV**) was obtained. Therefore, these IRC calculations clearly proved that **X** is the transition structure for the isomerization of **1** to **2**. At the UMP2/6-31G(d) and QCISD(T)/6-31G(d,p) levels of theory, **X** lies 23.7 and 22.9 kcal/mol, respectively, above **I**. Inclusion of the ZPVE correction in the latter value leads to an energy of activation at 0 K of 19.9 kcal/mol for the isomerization of **1** to **2** via **X**.

Formally, the propyl moiety of **X** can also be envisaged as the transition structure for the isomerization *n*-$C_3H_7^+$ → *sec*-$C_3H_7^+$ undergone by the incipient propyl cation formed by elongation of a terminal C−C bond in **1**. It is worthwhile to note that for the isolated propyl cation the isomerization *n*-$C_3H_7^+$ → *sec*-$C_3H_7^+$ occurs without an activation energy.[48] Therefore, the energy barrier of 19.9 kcal/mol predicted for the process **I** → **X** arises from the fact that the 1,2-hydrogen shift in the incipient propyl cation is synchronized with the C3−C4 bond cleavage, which is a structural change requiring a sizable amount of energy.

The energy of the transition structure **X** is calculated to be 3.6 kcal/mol *higher* than the sum of the energies of *sec*-propyl cation and methyl radical. Could there be a specific reason why the energy of **X** is higher than that of the separated dissociation fragments? The reason for this situation is traced to the fact that the $C_3H_7^+$ partner of **X** has a geometrical structure intermediate between those of *n*-$C_3H_7^+$ and *sec*-$C_3H_7^+$. Thus one would anticipate that the energy of the isolated $C_3H_7^+$ partner of **X** should be lower than that of the hypothetical *n*-propyl cation but higher than that of *sec*-propyl cation. In fact, at the QCISD(T)/6-31G(d,p) level of theory the energy of the isolated $C_3H_7^+$ unit of **X** was calculated to be 7.6 kcal/mol higher than that of *sec*-$C_3H_7^+$. Therefore, *it is concluded that the transition structure* **X** *is more energetic than the separated dissociation fragments sec*-$C_3H_7^+$ *plus* $CH_3^\bullet$ *because within its* $C_3H_7^+$ *unit the isomerization n*-$C_3H_7^+$ → *sec*-$C_3H_7^+$ *has not been fully accomplished yet.*

D. Elimination of $CH_3^\bullet$ and CH_4 from Ionized Isobutane. The MERP for the methyl radical elimination from **2** was calculated starting at the equilibrium structure **VII** using the long C−C bond distance (i.e., C2−C4) as the reaction coordinate, the energy being minimized with respect to all other geometrical variables without imposing any geometrical constraint. As the C2−C4 distance increased the C1−C2−C4 angle remained nearly unchanged, while the energy increased steadily. This path led to the dissociation of **2** to *sec*-$C_3H_7^+$ and $CH_3^\bullet$. At the UMP2/6-31G(d) level of theory, the sum of the energies of the separated fragments, *sec*-$C_3H_7^+$ and $CH_3^\bullet$, lies 21.9 kcal/mol above the energy of **VII**. At the QCISD(T)/6-31G(d,p) level, this dissociation energy is calculated to be 21.2 kcal/mol. The ZPVE correction reduces the dissociation energy to the value of 16.0 kcal/mol, which is reasonably close to the experimental estimate of 14.2 kcal/mol.[49]

Regarding the methane elimination from **2**, we note that at the highest level of theory the dissociation energy is calculated to be exothermic by 0.7 kcal/mol compared to an experimental value of 0.3 kcal/mol.[50] An extensive grid search using the C2−C4 distance and the C1−C2−C4 angle as reaction coordinates led to the location of an approximate saddle point at C2−C4 = 3.5 Å and C1−C2−C4 = 80°. The structure located in this way was refined by minimizing the scalar gradient of

(47) Schlegel, H. B. *J. Comput. Chem.* **1982**, *3*, 214.

(48) Raghavachari, K.; Whiteside, R. A.; Pople, J. A.; Schleyer, P. v. R. *J. Am. Chem. Soc.* **1981**, *103*, 5649.

(49) Estimated from $\Delta H^\circ_f(\mathbf{2})$ = 211.5 kcal/mol, ΔH°_f(*sec*-$C_3H_7^+$) = 190.9 kcal/mol, and $\Delta H^\circ_f(CH_3^\bullet)$ = 34.8 kcal/mol at 298 K.[44]

(50) Estimated from $\Delta H^\circ_f(\mathbf{2})$ = 211.5 kcal/mol, $\Delta H^\circ_f(CH_3CH{=}CH_2^{\bullet+})$ = 229 kcal/mol, and $\Delta H^\circ_f(CH_4)$ = −17.8 kcal/mol at 298 K.[44]

the energy using Schlegel's algorithm. The resulting optimized structure, **XI** (Figure 6), was characterized as a true transition structure by checking that it had only one imaginary harmonic vibrational frequency. The atomic displacements associated to the one imaginary frequency (112*i*) of **XI** consisted mainly in a lengthening of the C2−C4 distance combined with a decrease of the C1−C2−C4 bond angle. An IRC calculation beginning at the saddle point **XI** and proceeding in the direction corresponding to the shortening of the C2···C4 distance yielded a smooth path leading to the lowest-equilibrium structure calculated for **2**, namely **VII**. An IRC calculation starting at **XI** and proceeding in the direction corresponding to the lengthening of the C2···C4 distance gave a path leading to a local minimum, **XII** (Figure 7), which turned out to be a weakly bound ion-neutral complex between the propene radical cation and methane. Therefore, these IRC calculations verify that **XI** is the transition structure for the methane loss from **VII**.

At the transition structure **XI** the C1−H6 bond length is only 0.026 Å longer than its equilibrium value (1.102 Å) in **VII**, whereas the C4−H6 distance (2.544 Å) of the bond to be formed still is remarkably long. From this it appears that the methyl group to be eliminated has little methane character in the transition structure **XI**. Regarding the charge and spin density distributions, it is noteworthy that the sum of the total atomic charges of the propyl moiety (+0.969) accounts for nearly 97% of the positive charge of **XI**, whereas the sum of the total atomic spin densities of the methyl radical moiety (0.969) accounts for nearly 97% of the unpaired electron population of **XI**. Therefore, on the basis of the molecular geometry and the total atomic charges and spin densities, **XI** can be viewed as a *sec*-propyl cation coordinated to the methyl radical.

At the UMP2/6-31G(d) level, **XI** lies 17.2 kcal/mol above the equilibrium structure **VII**. This potential energy barrier is calculated to be 16.9 kcal/mol at the QCISD(T)/6-31G(d,p) level of theory. The inclusion of the ZPVE correction leads to a barrier of 12.9 kcal/mol. Recalling the calculated dissociation energy (16.0 kcal/mol) of **VII** to *sec*-$C_3H_7^+$ and $CH_3^\bullet$, **XI** is predicted to lie 3.1 kcal/mol *below* the energy of its loosely bound components.

Regarding the propene−methane ion−neutral complex **XII**, it is worth noting that the intermolecular distance C4···C2 between the two partners is 0.243 Å shorter than in the saddle point **XI**. At the QCISD(T)/6-31G(d,p) level, the energy of **XII** is predicted to lie 2.5 kcal/mol *below* the sum of the energies calculated for the separated components, propene radical cation and methane. Inclusion of the ZPVE correction to the latter value leads to a stabilization energy of **XII** toward dissociation into its loosely bound components of 1.8 kcal/mol. Since BSSE are expected to affect the computed interaction in the electrostatically bound complex **XII**, the latter stabilization energy value should be taken with caution.

E. Elimination of CH_4 and $CH_3^\bullet$ from Ionized Butane. The analysis of the results afforded from our exploration of the PES in the region concerning the unimolecular decompositions of **1** reveals that there is no MERP on the $C_4H_{10}^{\bullet+}$ ground-state PES for direct elimination of methane from this radical cation. Apparently, the methane loss from **1** is preceded by a mechanism requiring a prior elongation of a terminal C−C bond to a sufficient degree that the *n*-$C_3H_7^+ \rightarrow$ *sec*-$C_3H_7^+$ isomerization within the $C_3H_7^+$ partner can take place via the transition structure **X**. Subsequent methane elimination from the resulting methyl−propyl ion complex occurs through the lengthening of the long C−C bond to a point where the $C_3H_7^+$ partner can transfer a hydrogen atom to the $CH_3^\bullet$ partner via the transition structure **XI**. A comparison between the optimum geometries

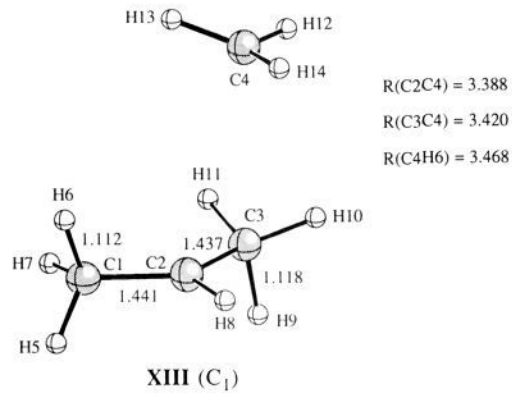

XIII (C_1)

Figure 8. UMP2/6-31G(d)-optimized geometry of the structure **XIII** on the IRC path **X** → **VII**.

calculated for the saddle points **X** and **XI** indicates that the most salient geometrical difference between them is the structure of the corresponding $C_3H_7^+$ partner. While in **X** the hydrogen atom H9 is nearly equidistant from the C2 and C3 carbon atoms, in **XI** this atom is exclusively bonded to the C3 carbon atom. Additionally, in going from **X** to **XI** the completion of the 1,2-hydrogen shift within the $C_3H_7^+$ partner is accompanied by a larger separation between the $C_3H_7^+$ and $CH_3^\bullet$ partners, as measured by the C3···C4 and C2···C4 distances. Interestingly, a close examination of the points found on the IRC path leading from **X** to **VII** showed that the C3···C4 distance increases along the first part of the pathway, reaching the maximum value of 3.420 Å, and then starts decreasing until it reaches its equilibrium value of 2.681 Å at the product **VII**. The structure (**XIII**) found by constrained geometry optimization for the point on this IRC with the largest C3···C4 distance is described in Figure 8. At the UMP2/6-31G(d) level of theory, the energy of **XIII** is calculated to lie 5.9 kcal/mol below that of the saddle point **X**. The C3−H9 bond length of 1.118 Å calculated for **XIII** indicates that at this stage of the IRC path the 1,2-hydrogen shift within the $C_3H_7^+$ partner has been completed, so its geometry is nearly identical to that of the isolated *sec*-propyl cation. Starting from this point on the IRC path, a non-IRC path was generated in internal coordinates (no mass weighting) with the UMP2/6-31G(d) wave function by varying the C4···H6 distance in small decrements, typically 0.1−0.2 Å, accompanied at each step by constrained optimization cycles for all other internal coordinates. This non-IRC path led to the equilibrium structure calculated for the ion−neutral complex **XII**. Similarly, a non-IRC path connecting the saddle point **X** and the dissociation fragments *sec*-C_3H_7 plus $CH_3^\bullet$ was generated in the same way by starting from **X** and varying the C2···C4 distance in small increments. As expected, the energy of both non-IRC paths stayed below that of the saddle point **X**.

It should be noted that a non-IRC path is not a steepest descent path and has no unique definition. As pointed out by Doubleday in a recent article,[51] the only significance of a non-IRC path is that it reveals an energetically accessible avenue to a non-IRC product, which by construction has the same accessibility as the IRC product. Furthermore, in the absence of classical trajectory calculations, an energetically accessible process must be taken seriously as a candidate for dynamical accessibility.[51] Thus, the **X** saddle point in addition to mediating the IRC path for the isomerization of **1** to **2** also mediates the losses of methyl radical and methane from **1**. This is illustrated in Figure 9, which is a schematic potential energy diagram based

(51) Doubleday, C., Jr. *J. Am. Chem. Soc.* **1993**, *115*, 11968.
(52) Derrick, P. J.; Donchi, K. F. *Comprehensive Chemical Kinetics*; Elsevier: Amsterdam, 1983, p 83.

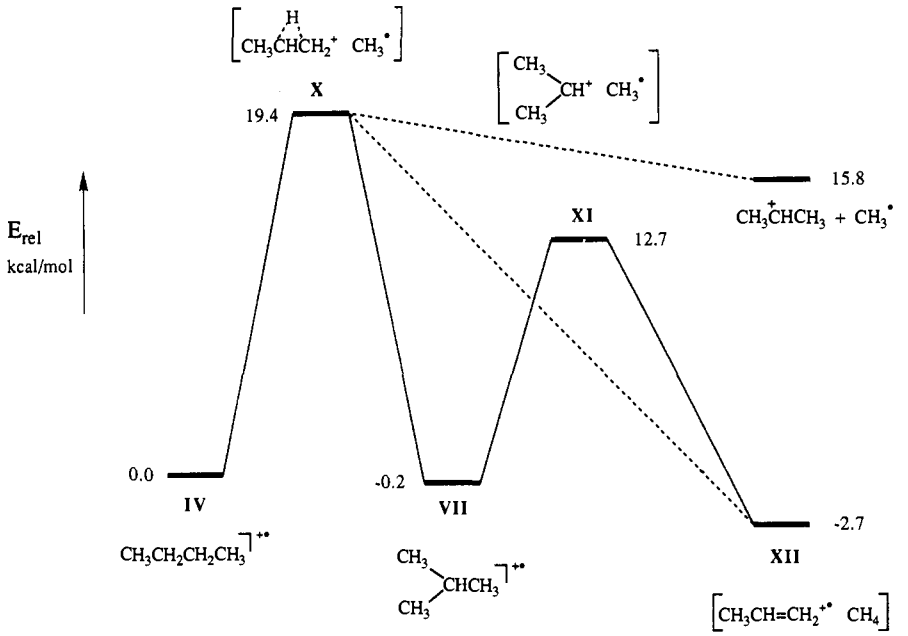

Figure 9. Schematic potential energy diagram showing the unimolecular reactions associated to IRC and energetically accessible non-IRC paths on the $C_4H_{10}^{\bullet+}$ ground-state PES. Energy values obtained from the ZPVE-corrected QCISD/6-31G(d,p) energies relative to that of **IV**.

Table 5. RRKM-Calculated Rate Constants (k, s^{-1}) and Rate-Constant Ratios as a Function of the Internal Energy (E, kcal/mol) for Loss of Variously Deuterated Methanes from Metastable $(CD_3)_2CHCH_3^{\bullet+}$ [a]

E	$k(CH_3D)$	$k(CD_4)$	$k(CD_3H)$	$k(CH_3D)/k(CD_4)$	$k(CH_3D)/k(CD_3H)$	$k(CD_3H)/k(CD_4)$
13.72	9.4×10^6	2.9×10^5	8.6×10^5	32.9	11.0	3.0
13.76	1.1×10^7	5.5×10^5	1.4×10^6	20.4	8.1	2.5
13.80	1.4×10^7	8.1×10^5	1.9×10^6	17.2	7.4	2.3

[a] E designates the internal energy above the ZPVE of the metastable radical cation.

on the relative energies calculated at the QCISD(T)/6-31-(d,p)+ZPVE level. The solid lines represent unimolecular reactions associated to IRC paths (i.e., **IV** → **X** → **VII** → **XI** → **XII**), whereas the broken lines represent unimolecular dissociation reactions associated with non-IRC paths (i.e., **X** → **XII** and **X** → *sec*-$C_3H_7^+$ plus $CH_3^{\bullet}$). It is worth noting that the loss of methane from **IV** does not actually require the molecule to go through the **XI** saddle point, because the non-IRC path is arbitrary and a variety of similar paths accomplish the same reaction. Figure 9 was drawn to show the choices that are energetically accessible to a path from saddle point **X**. In other words, *saddle point* **X** is *the transition state common to the isomerization of* **1** to **2** *and the elimination of both methane and methyl radical from* **1**. Then, transition state theories cannot predict the product ratio, other than a ratio of 1.[51] In any case, we suggest *that the energetically activated molecules of* **1** *can eliminate both methyl radical and methane without prior collapse to* **2**.

F. Comparison with Mass Spectrometry Experiments. As mentioned above in Sections C and D, on the basis of the calculated molecular geometries and total atomic charges and spin densities, the transition structures **X** and **XI** can be viewed as a H-bridged propyl (**X**) or *sec*-propyl (**XI**) cation, respectively, coordinated to the methyl radical. These results offer clear support to WBW's suggestion that methane loss from metastable ions **1** and **2** is mediated by ion−neutral complex species, in the sense of Scheme 1. In this particular case it turns out that such species are not local minima on the PES but saddle points which exhibit a small imaginary vibrational frequency. However, it should be noted that WBW developed the idea of ion−neutral complexes to describe reactions in which ions apparently dissociated to the point where the partners could react with each other or one of the partners could isomerize. Their complexes were not species confined to potential energy minima. On the other hand, the postulated ion−neutral complex **1a** (Scheme 1) involving coordination between the *n*-propyl cation and methyl radical is not even a stationary point on the PES, so it does not play any role in either the methane loss or the methyl radical elimination from metastable ions **1**.

Figure 9 is consistent with the mass spectrometry experimental findings reported in the literature. Thus, regarding the losses of methane and methyl radical from **1**, it is clear that the formation of the transition structure **X** constitutes the rate-determining step of both processes. This is in agreement with the fact that the appearance energies for the losses of methane and methyl radical from **1** are the same within experimental error.[7] Additionally, the about 6 kcal/mol lower threshold observed for the loss of methane than for the loss of methyl radical from **2**[10] is in acceptable agreement with the 3.1 kcal/mol energy difference found between the energy barrier of 12.9 kcal/mol, calculated for the methane elimination from **2**, and the dissociation energy of 16.0 kcal/mol, calculated for the dissociation of **2** to *sec*-propyl cation and methyl radical.

To investigate whether the sorts of changes in vibrational frequencies calculated for the transition structure **XI** are of the right magnitude to account for the observed[10] isotope effects associated with loss of variously deuterated methanes from metastable $(CD_3)_2CHCH_3^{\bullet+}$, rates of decomposition were calculated on the basis of the standard RRKM theory of unimolecular reactions. The unimolecular rate constants calculated at different internal energies (E) above the ZPVE of the metastable ions are summarized in Table 5. At the QCISD-(T)/6-31G(d,p) level, the potential energy barrier calculated for the methane loss from **VII** is 16.9 kcal/mol (see Table 2). However, due to the differences in the calculated ZPVE of the reactants and transition states involved in the various losses of

methane from $(CD_3)_2CHCH_3^{\bullet+}$, the energy threshold for CD_4 loss (13.72 kcal/mol), which is the methane loss showing the highest energy threshold, was taken as the minimum internal energy excess in the RRKM calculations. The relevant ratios of rate constants are also included in Table 5. Assuming that to a first approximation the relative intensities of metastable peaks for the various losses of methane are proportional to the rate constants of the rate-determining step of these processes,[52] then it follows that

$$\frac{k(CH_3D)}{k(CD_4)} = \frac{I(CH_3D)}{I(CD_4)} \quad (2)$$

$$\frac{k(CH_3D)}{k(CD_3H)} = \frac{I(CH_3D)}{I(CD_3H)} \quad (3)$$

$$\frac{k(CD_3H)}{k(CD_4)} = \frac{I(CD_3H)}{I(CD_4)} \quad (4)$$

where $I(CH_3D)$, $I(CD_4)$, and $I(CD_3H)$ are relative intensities for the losses of CH_3D, CD_4, and CD_3H, respectively. From the metastable peak intensities reported by Derrick and co-workers,[10] the experimental rate-constant ratios of 21.3, 8.5, and 2.5 are obtained from eqs 2, 3, and 4, respectively. These values are in excellent agreement with the rate-constant ratios of 20.4, 8.1, and 2.5, determined from the RRKM calculations at an internal energy of 13.76 kcal/mol (second row of Table 5), and lend further support to the reaction path predicted for the methane elimination from **2**.

Finally, we note that the observed[7] small amount of methyl radical and methane bearing an internal carbon atom eliminated from **1** is readily explained on the basis of the low-energy barrier (3.1 kcal/mol) predicted for the degenerate rearrangement in **2**, consisting of the exchange between one short C−C and the long C−C bond, as compared to the energy barriers predicted for the processes **I** → **X** (19.9 kcal/mol) and **VII** → **XI** (12.9 kcal/mol). Thus the amount of methyl radical and methane containing carbon atoms C2 or C3 eliminated from **1** should be roughly related to the degree of isomerization of **1** to **2** via the IRC path **X** → **VII** as compared to the non-IRc path **X** → **XII**.

IV. Conclusions

Our computational exploration of the $C_4H_{10}^{\bullet+}$ potential energy surface in the regions concerning the unimolecular decompositions of ionized butane and isobutane reveals several important points:

(1) A trans conformation structure (C_{2h} symmetry, ^2A_g electronic state) having a long central C−C bond is predicted to be the lowest-energy point on the ground-state PES of the butane radical cation. There is a second equilibrium structure (C_{2h} symmetry, ^2A_g electronic state) for the trans conformation that has a normal central C−C bond length and the terminal C−C bonds somewhat elongated, which is calculated to be 3.9 kcal/mol more energetic than the first one. At the UMP2/6-31G(d) level of theory, there is a transition structure for the interconversion of both equilibrium structures that lies 1.5 kcal/mol above the less energetic one.

(2) A gauche conformation structure (C_2 symmetry, ^2A electronic state), having a long central C−C bond, is also predicted to be a local minimum on the ground-state PES of the butane radical cation. This structure is calculated to be 0.5 kcal/mol more energetic than the lowest-energy trans conformation. Both minima are connected via a transition structure (C_2 symmetry) lying 2.0 kcal/mol above the trans isomer.

(3) A cis conformation structure (C_{2v} symmetry, $^2A_1$ electronic state), also having a long central C−C bond, is predicted to be a saddle point on the ground potential energy surface of the butane radical cation. This is the transition state for the interconversion of the two equivalent gauche conformations. The energy barrier for this process is calculated to be 3.1 kcal/mol.

(4) The lowest-energy point on the ground potential energy surface of the isobutane radical cation is a structure (C_s symmetry, $^2A'$ electronic state) having a long C−C bond and two somewhat short C−C bonds. This structure is calculated to be 0.3 kcal/mol more energetic than the lowest-energy trans isomer of the butane radical cation. There is a second equilibrium structure (C_s symmetry, $^2A''$ electronic state) showing two lengthened C−C bonds and a somewhat short C−C bond. The latter structure is calculated to be 4.1 kcal/mol more energetic than the first one. At the UMP2/6-31G(d) level of theory, there is a transition structure for the interconversion of both equilibrium structures that lies 2.6 kcal/mol above the less energetic one. The degenerate rearrangement, consisting of the exchange between the long C−C bond and one of the two short C−C bonds in the lowest-energy equilibrium structure, takes place via a two-step mechanism which involves the formation of the more energetic equilibrium structure as an intermediate along the path. The low-energy barrier calculated at all levels of theory indicates that scrambling of the methyl groups in isobutane radical cation should be a facile process.

(5) The isomerization of ionized butane to the isobutane radical cation takes place via a transition structure lying 19.9 kcal/mol above the lowest-energy trans conformation of ionized butane and 3.6 kcal/mol above the sum of the energies calculated for the separated *sec*-propyl cation and methyl radical. On the basis of the calculated molecular geometry and the atomic charges and spin densities distribution, this transition structure can be viewed as a nonclassical H-bridged propyl cation coordinated to the methyl radical. In addition to mediating the isomerization of ionized butane to the isobutane radical cation, this transition state also mediates the losses of both methyl radical and methane from ionized butane through non-minimum-energy reaction paths which are energetically accessible. Therefore, energetically activated molecules of ionized butane may eliminate both methyl radical and methane without prior collapse to the isobutane radical cation. Consequently, the formation of the above transition structure constitutes the rate-determining step of both eliminations.

(6) The loss of methane from ionized isobutane is predicted to take place via a transition structure lying 12.9 kcal/mol above the lowest-energy equilibrium structure of this radical cation. On the basis of the calculated molecular geometry and the atomic charges and spin densities distribution, this transition structure can be viewed as a *sec*-propyl cation coordinated to the methyl radical. Since the sum of the energies of the separated *sec*-propyl cation and methyl radical is calculated to be 3.1 kcal/mol higher than the energy of this transition state, the methane loss from ionized isobutane requires a lower activation energy than methyl radical elimination.

(7) The present results give support to WBW's suggestion that methane loss from metastable butane and isobutane radical cations is mediated by ion−neutral complex species. However, it turns out that in this particular case such species are not local minima on the PES but saddle points, which possess a small imaginary vibrational frequency. On the other hand, the ion−neutral complex involving coordination between an *n*-propyl

cation and the methyl radical, postulated by WBW, is not even a stationary point on the PES.

Acknowledgment. This work was supported by the Robert A. Welch foundation (Grants H-609 and BD-1106) and the Spanish DGICYT (Grant PB89-0256). The preliminary UHF calculations were carried out by one of us (S.O.) in the Department of Marine Sciences (Texas A&M University at Galveston), during his stay in the summer of 1991, which was partially supported by the Catalonian CIRIT foundation. We acknowledge the University of Texas Center for High Performance Computing and the Centre de Supercomputació de Catalunya for generous allocations of computing time. We also acknowledge helpful discussions with Dr. Charles Hudson from the Marine Biomedical Institute and Professor Antonio Aguilar from the University of Barcelona.

Supplementary Material Available: Tables showing the UMP/6-31G(d) optimized geometries for the stationary points calculated on the ground-state PES of the butane and isobutane radical cations (6 pages). This material is contained in many libraries on microfiche, immediately follows this article in the microfilm version of the journal, and can be ordered from the ACS; see any current masthead page for ordering information.